Environmental Earth Sciences (2021) 80:814
https://doi.org/10.1007/s12665-021-10064-3

THEMATIC ISSUE

Petrophysical properties of limestones: influence on behaviour under different environmental conditions and applications

Luís Sousa[1] · Johanna Menningen[2] · Rubén López-Doncel[3] · Siegfried Siegesmund[2]

Received: 30 August 2021 / Accepted: 16 October 2021 / Published online: 29 November 2021

Abstract

Limestones are of wide variety, namely with differences in the process of formation, mineralogical composition, grain size and texture. Such variability leads to differences in weathering characteristics and behaviour under different environmental conditions and applications. Therefore, detailed studies are mandatory to assess the main factors controlling the physical–mechanical properties and durability to propose the best applications for limestones. This study presents the petrographic and petrophysical data of 11 selected Portuguese limestones. Texture, mineralogy and porosity were identified as key parameters for the durability of limestones. Two main groups were identified regarding the texture/petrography and weathering resistance: the compact micritic limestones and with the sparitic grainstones. For the first time an outstanding bowing behaviour was identified in a limestone, probably related with clay swelling minerals and iron oxides present in the micrite groundmass around or in the stylolitic planes.

Keywords Limestones · Textural characteristics · Durability · Weathering resistance · Bowing

Introduction

Building stones have a high range of applications and worldwide production show an increasing tendency based on continuous research on several related topics (Yarahmadi et al. 2018, 2019a; Montani 2017). In the past, aesthetic properties were the first factor in building stone selection (Sousa et al. 2016; Santos et al. 2018), while the petrophysical properties were of secondary importance. The knowledge about the interference of the stone properties in weathering and durability behaviour when employed in buildings has increased substantially in the last decades. Many researches point out the problems raised by misinformation about building stones and related conservation issues, especially in highly porous materials (Unterwurzacher and Mirwald 2008; Siegesmund et al. 2010; Espinosa-Marzal et al. 2011; Stück et al. 2013; Wedekind et al. 2013; Molina et al. 2015; López-Doncel et al. 2016).

Limestone is probably a building stone type with a wide variety range, namely with differences in the process of formation, mineralogical composition, grain size and texture. Such variability of the carbonate rocks leads to differences in weathering characteristics and behaviour under different environmental conditions and applications (Freire-Lista et al. 2021). Textural and porous properties are the main factors ruling stone behaviour, but weather conditions will enhance the degradation of the highly porous materials. Barnoos et al. (2020) mention the presence of secondary calcite veins and clay veins in the microstructure of a limestone as cause for delamination and fragmentation and washing out during exposure to water, respectively. Yagiz (2011) identified random microcracks infilled with calcite, which makes the rock weaker than anticipated. The abrasion resistance is influenced by the internal structure of rock samples being lower when cracks, gaps and large fossils are present

This article is part of a Topical Collection in Environmental Earth Sciences on "Building Stones and Geomaterials through History and Environments—from Quarry to Heritage. Insights of the Conditioning Factors", guest edited by Siegfried Siegesmund, Luís Manuel Oliveira Sousa, and Rubén Alfonso López-Doncel.

✉ Luís Sousa
lsousa@utad.pt

[1] Department of Geology and Pole of CGeo - Geoscience Center, University of Trás-os-Montes e Alto Douro (UTAD), Vila Real, Portugal

[2] Geoscience Center of the University Gottingen, Gottingen, Germany

[3] Geological Institute of the Autonomous University of San Luis Potosí, San Luis Potosí, Mexico

(Özvan and Direk 2021). Nasri et al. (2019) point out the importance of bioturbation, fissures, micro- and macroporosity in weathering characteristics and stone durability of limestone and carbonate tufa. Korkanç et al. (2021) studied a monument where a hard and low porous limestone did not appear to have sustained damage over thousands of years due to environmental conditions. With increasing acidity, the rate of weathering increases, and the mechanical properties decrease as pointed out by Fereidooni and Khajevand (2019) in accelerated weathering tests.

The physico-mechanical properties (PMP) reflect the variability of the limestones, especially the porosity and the compressive strength. Siegesmund and Dürrast (2014) in a statistical evaluation mention values of uniaxial compressive strength (UCS) in limestones ranging from 4.4 MPa to 265 MPa and porosity values from < 1% to > 20%. Arman et al. (2021) show data of rock strength of carbonate rocks with a wide range of variability and propose the derived correlation equations of the rock strength parameters. Despite the wide range of values for the physical–mechanical properties of limestones, some relationships are common. The P-wave, UCS and density change jointly, while the thermal conductivity has a negative correlation with porosity (Siegesmund and Dürrast 2014; Yaşar et al. 2008). These relationships help to select the best application (floor, façade, inside, outside, …) for each material to maximize the properties in which the selection was made.

The knowledge of the PMP of stones used in heritage monuments is a critical issue, both to know the constraint factors dominating the evolution under specific environmental conditions and predict the durability and span of life of the buildings, and to choose the best solution when repairing works are necessary. The identification of the PMP of building stones can lead to their better maintenance and safekeeping (Taghipour et al. 2017; Korkanç et al. 2021), avoiding the use of inappropriate restoration material (Barnoos et al. 2020). When repairing or replacement of damaged stones is necessary, the best option is to use stones with similar properties from the original ancient quarries (Taghipour et al. 2017). Conservation based on artificial products should always maintain the resistance and appearance of the original material (Agan 2016).

The competitiveness in the building stone industry demands a clear picture of the possibilities of the different uses for each stone, point outing the qualities but also the limitations (Carvalho et al. 2013; Mustafa et al. 2016; Yarahmadi et al. 2019b). Different purposes such as new construction or monument rehabilitation demand detailed information to ensure the best choice. A wrong application can have consequences for the image of a building stone that are hard to revert. Decades of marketing diplomacy can be destroyed by a single building where the stone was not judiciously selected. The above-mentioned factors, from texture to mechanical properties, should always be considered as critical information. In this line, in the present research 11 varieties of Portuguese limestones covering a wide range of textures and PMP were used. The main objective is to highlight the main factors controlling the physical–mechanical and durability behaviour and propose the best applications for limestones. The systematic evaluation of the factors controlling Portuguese limestone behaviour has never been done with such a number of samples. Besides the insights into the rock properties, the results will be helpful to focus the communication target of limestone producers and traders.

Materials and methods

The limestone samples used in this study were collected from the Maciço Calcário Estremho (MCE), a Jurassic limestone massif located in the Portuguese Lusitanian Basin, except for one sample (LIOZ) collected from a Cretaceous Unit near Lisbon (Silva 2017) (Fig. 1).

MCE is one of the world's leading region producers of limestone for ornamental purposes (Carvalho and Lisboa 2018). The quarries developed along the hillside, with several benches, can reach depths around 50 m and are grouped exploitation sites (Fig. 1) (Carvalho and Lisboa 2018). Several lithostratigraphic units are exploited and give rise to different ornamental varieties, from cream laminated calcarenites to grey calciclastic micritic limestones. The samples selected from MCE show this high variability. The following commercial varieties were selected: Alpinina (ALP), Ataíja Azul (ATAZ), Ataíja Creme (ATCR), Semi-rijo Codaçal (cut parallel to the sedimentary lamination, CODFV), Lioz (LIOZ), Moca 4 M (cut perpendicular to the sedimentary lamination, MCCT), Semi-rijo Branco Mais(i) (SBM), Semi-rijo Branco Real (SBR), Vidraço Azul Valverde (VAV); Vidraço Portela Azul (VPAZ); Vidraço Portela Creme (VPCR). From hereon, the designations used are the ones indicated in brackets.

The limestones present different hues from beige to brown, according to the size of the bioclast and intraclast particles and cement constitution. Aleatory or laminated distribution of their constituents imprints a remarkable heterogeneity to some limestones. Most of the studied limestones show a light beige hue, and only ATAZ, VPAZ and VAV samples have dark hues (Fig. 2).

Thin sections were used to perform the petrographic studies. X-ray diffraction of whole-rock samples was used to determine the mineralogical and geochemical composition. The following properties of the studied limestones were evaluated: density, porosity, capillary water absorption, pore radii distribution, ultrasound velocity, thermal expansion, bowing potential, thermal shock, and salt burst tests. The general description of the methods is given below.

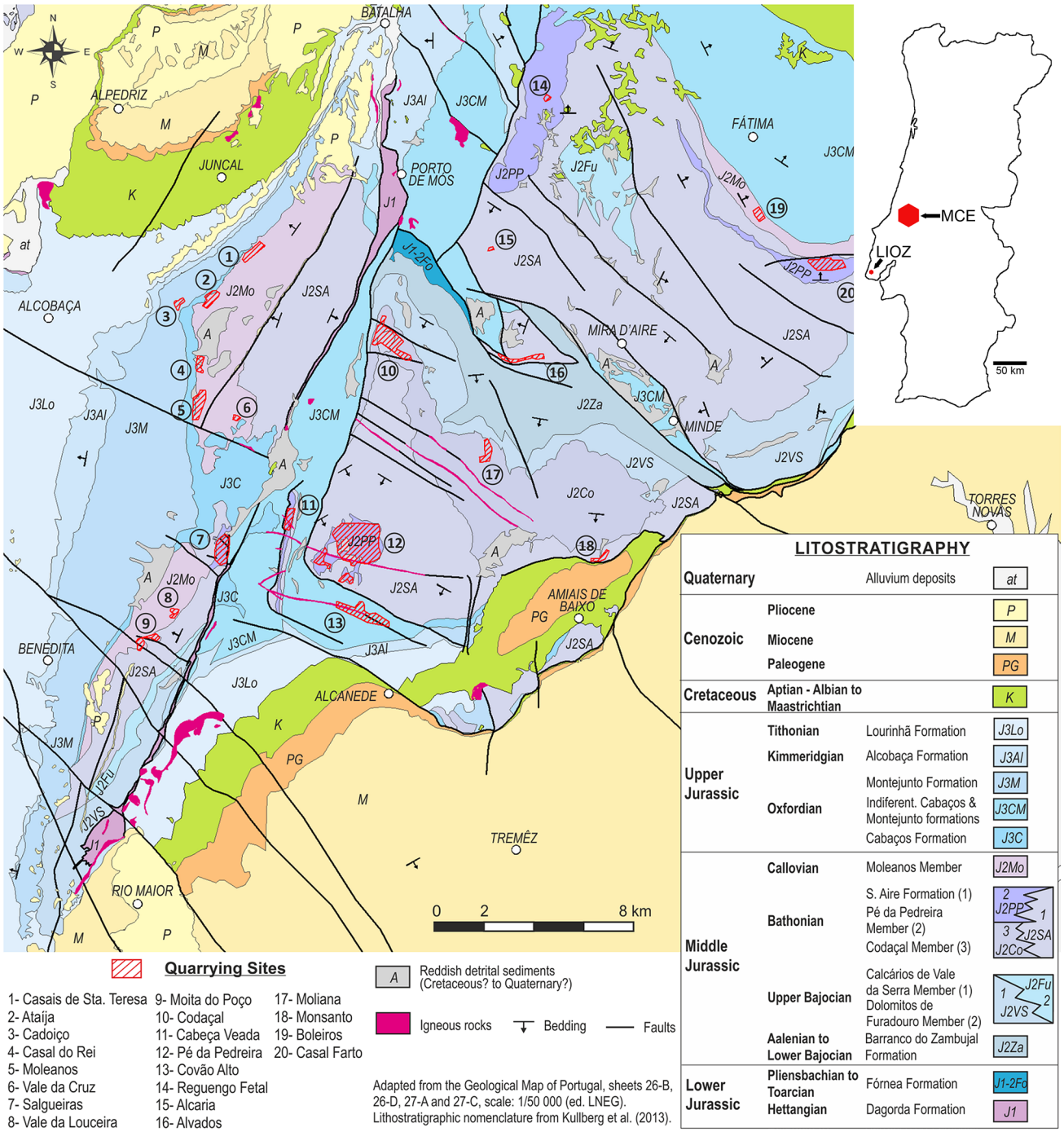

Fig. 1 Location of the samples from the Maciço Calcário Estremenho (MCE) and LIOZ sample. Lithostratigraphic map of the MCE with the locations of quarrying sites (map modified from Carvalho and Lisboa 2018). MCE samples were collected in the following quarrying sites: 1, 2, 7, 8, 10, 12 and 18

Open porosity and density were measured in 6.5 cm cubic samples using the hydrostatic weighting method (DIN 52,102). The water-saturated mass and the buoyancy mass of the samples were measured after water saturation under vacuum and the dry mass was used to calculate the porosity.

The capillary water absorption was measured on cubic samples with dimensions of 6.5 cm in length. The bottom plane of the cubes was placed in water (until a meniscus formed surrounding the entire sample) and the weight increase was measured.

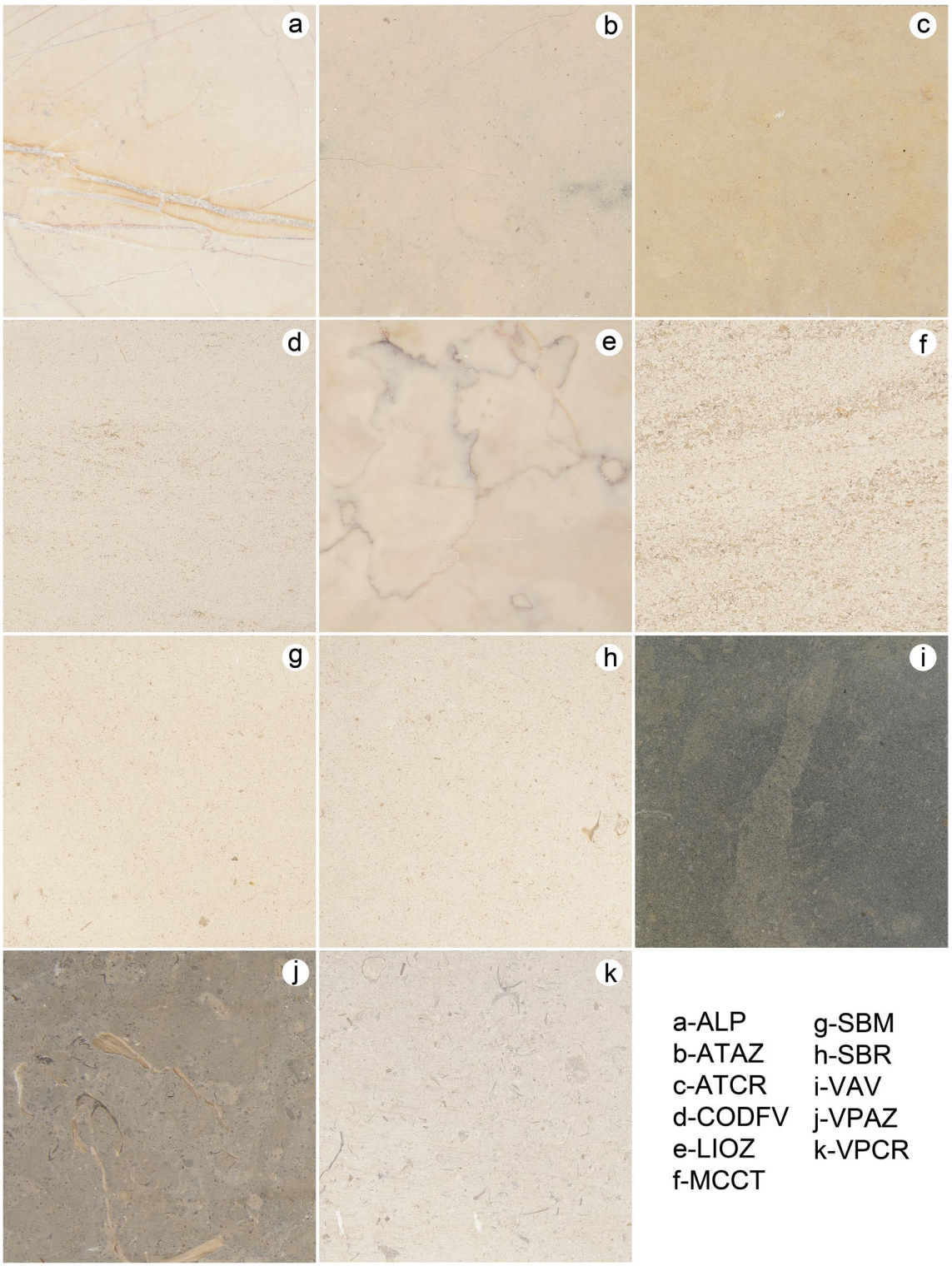

Fig. 2 Macroscopic appearance of the studied limestones (honed surfaces; size of the pictures: 10 cm × 10 cm)

The pore size distribution was measured by mercury intrusion porosimetry (MIP; Pascal 140 and Pascal 440 from Thermo Scientific) using irregular samples (ca. 1.0–1.5 g). Pressures up to 400 MPa were used to evaluate the pore radii measured at around 0.005 µm.

Ultrasound measurements were performed using the compressional wave velocity. The Geotron Ultrasound generator USG 40 and the Oscilloscope Fluke Scope Meter 192 were used according to DIN EN 14,579:2004. The examinations were carried out with a frequency of 350 kHz on 3 cubes per sample for three orthogonal measurements and a mean of nine measurements on dry and wet samples.

Thermal expansion measurements were performed in the temperature range of 20 °C–90 °C using a pushrod dilatometer (for details see Strohmeyer 2003; Koch and Siegesmund 2004). Heating and cooling were performed with a velocity of 1 °C/min. The residual strain (εRS) was determined during seven heating–cooling cycles: three dry cycles 20–90–20 °C; four wet cycles 20–90–20 °C. εRS is determined by the ratio between the sample length change after the heating–cooling cycles and the initial length (for details see Weiss et al. 2004; Zeisig et al. 2002; Shushakova et al. 2013).

To determine the bowing potential and its directional dependence, slabs of 40 × 10 × 3 cm were exposed to heating cycles (20–80–20 °C per day), according to DIN EN 16,306:2013–05, simulating in an extreme way the conditions at the building. Additionally, specimens were exposed to thermo-hygric cycles, moisture on one side (samples lying on an mm-thick film of demineralized water) and cyclical heat from a heating pad 3 cm above the slab surface on the reverse side. One cycle included a heating period of 5 h, where the surface finally reached 80 ºC and a cooling period of at least 12 h, so that the duration of one cycle was 1 day. The bowing was measured using a measuring bridge with an accuracy of 1 µm/35 cm every first to the fourth cycle (see Koch and Siegesmund 2002, 2004; Grelk et al. 2004). A total of 105 cycles were performed.

Thermal shock test was performed in cubic samples with dimensions of 6.5 cm in length. After a period of about 16 h in the oven at high temperatures (100 ºC and 200 ºC), the samples were cooled in water at 10 ºC for 8 h. A total of 34 cycles were completed, 18 at 100 ºC and 16 at 200 ºC. The samples were visually examined after each cycle and monitored with ultrasound measurements, performed after several cycles, before the samples dried completely at 60 ºC. One cube per sample was used and the ultrasound value was taken from the mean value of three orthogonal measurements.

The salt crystallization test was performed according to the standard DIN EN 12,370. The samples (5 cm cubes) were soaked in a 10% Na_2SO_4 solution. The samples were submerged for about 4 h in the solution and then dried in an oven at 60 °C for 16 h. After cooling to room temperature for 4 h, the cubes were weighed to determine the loss of material.

Results and discussion

Petrography, mineralogy and geochemistry

The thin section observations allow the identification of the main petrographic characteristics of the studied limestones, which are summarized below and illustrated in Fig. 3.

ALP—tectonized micritic limestone with oncolits; slight recrystallized and red stylolitic planes and calcite veins are remarkable features (Carvalho 2013).

ATAZ—this variety is very compact with a uniform texture, presenting frequent bioclasts of small size (Carvalho 2013).

ATCR—similar to ATAZ with a cream hue. When impregnated by yellowish hydrated iron oxides, the peloids can produce different hues (Carvalho et al. 2018).

CODFV—bioclastic and oolithoclastic grainstone with abundant sparitic cement. A sedimentary lamination, visible by differences in grain size, is a common feature (Fig. 3c). Large pores are frequent.

LIOZ—microcrystalline, bioclastic, fossiliferous limestone. The fossil content of rudist is a remarkable feature of this stone (Silva 2017).

MCCT—this sample is made of coarse intraclasts and bioclasts and a variable amount of peloids, with abundant sparitic cement (Carvalho 2013; Carvalho et al. 2014). It shows evident lamination from alternating levels of different grain sizes and compositions (Fig. 3a). Large spheroidal or ellipsoidal pores are frequent.

SBR—biolithoclastic limestone, with fine to coarse peloids and ooids. Large spheroidal or ellipsoidal pores are frequent.

SBM—similar to SBR samples with a lighter hue. The outermost part of the peloids are slightly impregnated by yellowish hydrated iron oxides.

VPAZ—micritic limestone with some marl content, occasionally oolitic, peloidal or intraclastic and bioclastic rich.

VPCR—similar to VPAZ but with coarser bioclastic content; consequently, has a lighter hue than the VPAZ sample.

VAV—micritic limestone with ooids, oncoids and bioclasts. Alternating levels with a variable proportion of allochemical components can be observed. Some iron-rich lines are observed in the packstone levels (see right side of Fig. 3f).

In Table 1 the main characteristics of the selected limestones are presented, as well as their classification according to Dunham (1962) and Folk (1962).

The pores are more frequent in the MCCT, CODFV, SBR and SBM samples, occurring dispersed in the thin

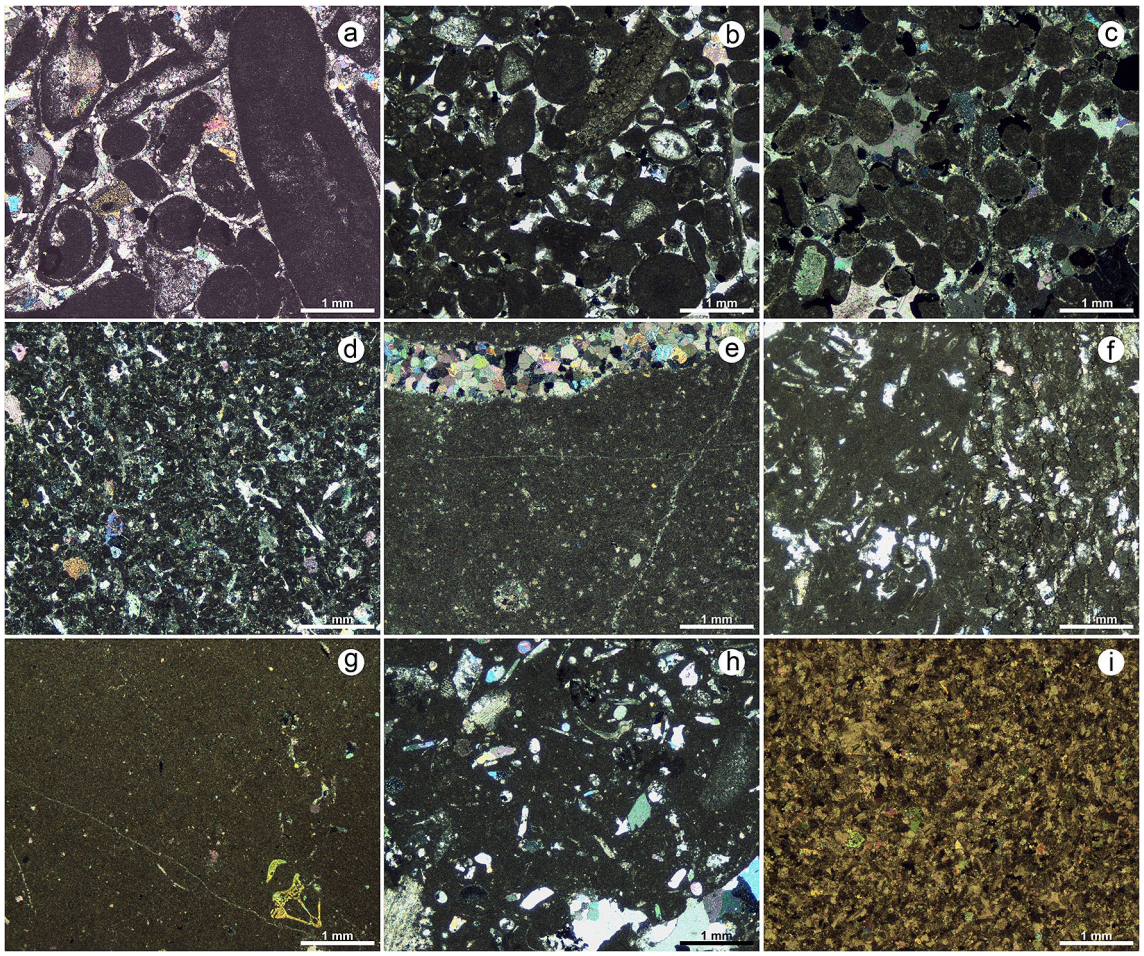

Fig. 3 Microscope appearance of the studied limestones (**a** MCCT; **b** SBR; **c** CODFV; **d** ATAZ; **e** ALP; **f** VAV; **g**VPAZ; **h**VPCR; **i** LIOZ)

sections. They are usually isolated spheroidal within the sparry cement and sometimes arranged as a circular crown around the allochemical components (Carvalho et al 2018). The mean pore size is between 50 µm and 200 µm in limestones from MCE (Carvalho et al 2018); however some larger pores were observed and could have originated during the thin section preparation.

These observations, namely the porosity, grain size, matrix and cement type (micrite/sparite) and allochems allow a first approach to the strength of the stones. Micrite and dolomite affect the mechanical parameters positively, while sparite and allochems decrease the strength parameters (Akram et al. 2017). Limestones with small crystals have a higher energy consumption during the wear than a macrocrystalline limestone, because the crack needs to pass more crystal boundaries which have a greater strength compared to cleavage planes (Jensen et al. 2010). Impurities such as clay minerals decrease the strength and cause sudden changes in the microporous network characteristics and consequently vary the durability of the building stone (Tugrul and Zarif 2000; Jensen et al. 2010; Zammit and Cassar 2017).

The chemical composition of the studied limestones is very similar, with small differences (Table 2). The VAV limestone stands out showing a high quantity of magnesium and dolomite. In fact, VAV limestone shows a calcite percentage of 90.9, whilst the other limestones have values between 94.5% and 98.4%. With magnesium carbonate, the opposite happens: VAV—4.8%; others—1.3%–2.6%. These results are according to the information available in the Catalogue of Portuguese Ornamental Stones (Leite and Moura 2021).

Density, porosity, and pore radii

The bulk density varies slightly between 2.61 and 2.71 g/cm^3 in eight samples and is lower 2.22–2.39 g/cm^3 in four samples because of the higher percentage of void space (Table 3), in accordance with published data (Matović and Ćalić 2016; Siegesmund and Dürrast 2014). Oolitic

Table 1 General characteristics and classification of the selected limestones (according to Dunham (1962) and Folk (1962))

Sample	General characteristics	Classification
ALP	Grey limestone composed of a micritic matrix (95%) and 5% of components	Pelagic mudstone (after Dunham, 1962) and micrite (after Folk 1962)
ATAZ	Light cream limestone with 50% groundmass and 50% components	Peloidal wackestone (after Dunham, 1962) and pelmicrite (after Folk 1962)
ATCR	Cream coloured limestone with 60% groundmass and 40% components	Peloidal wackestone and packstone (after Dunham, 1962) and pelmicrite (after Folk 1962)
CODFV	Light grey limestone composed of 60% sparry calcite cement and 40% components	Ooid–peloid grainstone (after Dunham, 1962) and oopelsparite (after Folk 1962)
LIOZ	Fully recrystallized limestone composed of dolomite microcrystals (dolosparite and dolomicrosparite)	Dolosparite (after Folk 1962)
MCCT	Light cream limestones composed of 50% sparite cement and 50% components	Bioclastic grainstone (after Dunham, 1962) and biopelsparudite (after Folk 1962)
SBM	Light cream limestone composed of 40% groundmass and 60% components	Peloidal grainstone (after Dunham, 1962) and Pelsparite (after Folk 1962)
SBR	Light cream limestone composed of 40% groundmass and 60% components	Ooid grainstone (after Dunham, 1962) and oosparudite (after Folk 1962)
VAV	Light to medium grey limestone composed of 70% groundmass and 30% components	Bioclastic packstone/grainstone (after Dunham 1962) and Biosparite/biodismicrite (after Folk 1962)
VPAZ	Medium grey limestone composed of a micritic matrix (> 90%) and less than 10% of components	Pelagic mudstone (after Dunham, 1962) and micrite (after Folk 1962)
VPCR	Light grey limestone composed of 60% groundmass and 40% components	Bioclastic floatstone (after Dunham, 1962) and biomicrudite (after Folk 1962)

Table 2 Chemical composition of the limestones (values in percentage)

	ALP	ATAZ	ATCR	CODFV	LIOZ	MCCT	SBM	SBR	VAV	VPAZ	VPCR
CaO	55.47	54.53	54.42	55.33	55.22	55.43	55.34	55.42	52.39	53.79	54.34
MgO	0.23	0.33	0.31	0.33	0.26	0.29	0.34	0.31	1.04	0.57	0.51
SiO_2	0.13	0.59	0.84	0.1	0.34	0.05	0.09	0.05	1.46	1.06	0.71
Fe_2O_3	0.05	0.18	0.16	0.05	0.05	0.05	0.07	0.04	0.3	0.14	0.13
Al_2O_3	0.08	0.38	0.45	0.06	0.12	0.03	0.05	0.03	0.42	0.38	0.3
K_2O	0.02	0.03	0.03	0.01	0.01	0	0.01	0	0.08	0.03	0.03
Mn_2O_3	0.02	0.02	0.02	0.01	0.01	0.01	0.01	0.01	0.02	0.01	0.01
Na_2O	0.08	0.01	0.02	0.01	0	0	0.07	0	0.03	0.02	0.02
SO_3	0.23	0.293	0.077	0.038	0.025	0.034	0.039	0.036	0.663	0.346	0.118
CO_2	43.3	42.86	42.83	43.47	43.54	43.59	43.54	43.7	42.26	42.69	43.09
H_2O	0.37	0.55	0.75	0.39	0.34	0.3	0.3	0.29	1.24	0.82	0.57
Total	99.980	99.773	99.907	99.798	99.915	99.784	99.859	99.886	99.903	99.856	99.828
$CaCO_3$	98.391	96.466	96.319	97.893	97.870	98.171	97.886	98.103	90.886	94.550	95.680
$MgCO_3$	1.052	1.509	1.418	1.509	1.189	1.326	1.555	1.418	4.757	2.607	2.333
$CaCO_3 + MgCO_3$	99.443	97.975	97.737	99.402	99.060	99.497	99.441	99.521	95.642	97.157	98.013

limestones show the lowest values as previously pointed out by Siegesmund and Dürrast (2014). The real or matrix density is close to the density of calcite, as is usual since it is the main component of the limestones studied (Matović and Ćalić 2016).

The values of porosity show a wide range, from 0.11% in LIOZ limestone to 18.80% for the SBM variety, reflecting the span of rock types and related textures. These values of porosity are only valid for the studied samples and can be used as an approximated value for the limestone varieties, since changes in the microporous network characteristics with depth of extraction have been reported (Tugrul and Zarif 2000; Zammit and Cassar 2017). Some varieties extracted in the MCE were previously studied and the porosity values range from 1.8% to 17.7% (Alves et al. 2011; Carvalho et al. 2018). Even the companies mention high

Table 3 Obtained values of porosity, bulk density, matrix density and capillary water absorption (CWA)

Stone	Bulk density (g/cm^3)	Mtx density (g/cm3)	Porosity (%)	CWA ($Kg/m^2h^{1/2}$)
ALP	2.70	2.71	0.55	0.55
ATAZ	2.69	2.70	0.47	0.37
ATCR	2.67	2.70	1.17	0.86
CODFV	2.28	2.71	16.11	2.94
LIOZ	2.71	2.71	0.11	0.38
MCCT	2.39	2.71	11.94	1.59
SBM	2.22	2.71	18.80	5.50
SBR	2.35	2.71	13.48	3.05
VAV	2.64	2.71	1.27	0.81
VPAZ	2.64	2.69	2.27	0.63
VPCR	2.61	2.71	3.87	0.39

values of porosity for some of the varieties exploited in MCE (Solancis 2021).

Textural characteristics control the porosity, therefore micritic varieties have lower values than the detritical varieties, which display intergranular voids (Benavente et al. 2015; Ruffolo et al. 2017). Reflecting the textural properties in limestones, a wide range of values of porosity can be found in literature, from values lower than 2% (Hashemi et al. 2018; Majeed et al. 2020; Hu et al. 2020; Korkanç et al. 2021) to values higher than 30% (Turgut et al. 2008; Eslami et al. 2010; La Russa et al. 2013; Szemerey-Kiss and Török 2017; Van Stappen et al. 2019; Zenah et al. 2020). The high variability of the porosity of limestones indicates their durability, because porosity is an excellent indicator of weathering (Tugrul and Zarif 2000) and strength properties (Nasri et al. 2019; Nabawy and El Aal 2019). As porosity is the key factor controlling most of the petrophysical properties and durability, the samples CODFV, MCCT, SBM and SBR probably will be less resistant to weathering.

The pore radii distribution, porosity and water absorption are important parameters in stone conservation studies, being related to stone weathering resistance (Siegesmund and Dürrast 2014). Results from mercury intrusion show the pore access radii (Vázquez et al. 2013) meaning that pores not interconnected will not be recognized, while the cracks are accounted as pores. Furthermore, some disturbance occurs during the injection of the mercury and the porosity values will be higher than those obtained by hydrostatic weighting (Freire-Gormaly et al. 2015; Anovitz and Cole 2015; Sousa et al. 2017). From the several pore size classification schemes (Vásquez et al. 2013; Siegesmund and Dürrast 2014), the following was used: pores lower than 0.1 µm (micropores); pores higher than 0.1 µm (capillary pores and macropores) (Klopfer 1985; Sousa et al. 2018). The pore sizes show an unequal bimodal distribution (see Ruedrich and Siegesmund 2007) with most of the pores distributed in the range between 0.01 µm and 0.8 µm and some pores with 10–50 µm (Fig. 4). Some samples exhibit a slight tendency to a polymodal pore size distribution as pointed out by Nasri et al. (2019). According to Vásquez et al. (2013), the smallest pores (< 0.1 µm) are related with intragranular porosity, the largest pores (> 10 µm) represent the intergranular porosity and the intermedium size (around 1 µm) is the matrix porosity. The values of the pore access radii are low, with a mean value between 0.015 µm and 0.298 µm, and mode values showing higher values from 0.08 µm to 0.53 µm (Table 4). Clastic and most porous varieties (CODFV, MCCT, SBM and SBR) have larger pore sizes, showing some intercrystalline porosity in the sparitic groundmass. The same samples have a higher percentage of macroporosity (82.7–90%), while the other samples show a higher microporosity (73.1–95.4%). Besides a higher total porosity, the most porous samples have a higher potential of water absorption, with larger pores.

The values of pore access radii identified in previous researches show a wide range of values, according to the textural characteristics, pore network and methodology used in the determination (Vásquez et al. 2013; Benavente et al. 2015; Freire-Gormaly et al. 2015; Török and Szemerey-Kiss 2019; Hu et al. 2020).

Water absorption and hydric expansion

The dynamics of the absorption is similar for the stones (Fig. 5), but only the most porous (e.g., CODFV, MCCT, SBM and SBR) show high water absorption. Within the first hours, the absorption of water is more evident and tends to stabilize after 6–9 h, depending on the porous interconnectivity. After 24 h the most porous samples show water uptake values in the range of 8.1–11.2 kg/m^2 and the others in the range of 0.2–0.6 kg/m^2. The sample SBM, with the highest porosity, reaches 100% of the weight absorption in 4 h, revealing a good connection of the porous network. The water absorption is connected to the porosity and similar curves can be found in different types of rocks, but the size and connectivity of the pores affect the rate of absorption (Çelik and Kaçmaz 2016; Karagiannis et al. 2016; Feijoo et al. 2017; Sousa et al. 2018; Barroso et al. 2018). Sedimentary layering, stylolites, microfractures and heterogeneous microfabric impact the kinetics of water absorption in limestones (Tomašić et al. 2011; Siegesmund and Dürrast 2014; Zenah et al. 2020). As mentioned for porosity, CWA values show a wide range of values which are according to the published results (Siegesmund and Dürrast 2014; Vásquez et al. 2013, 2015; Benavente et al. 2015). Capillary water absorption (CWA) is higher in the porous samples (e.g., CODFV, MCCT, SBM and SBR) with values between 1.59 and 5.50 $kg/m^2h^{1/2}$, and lower in the remaining samples, ranging

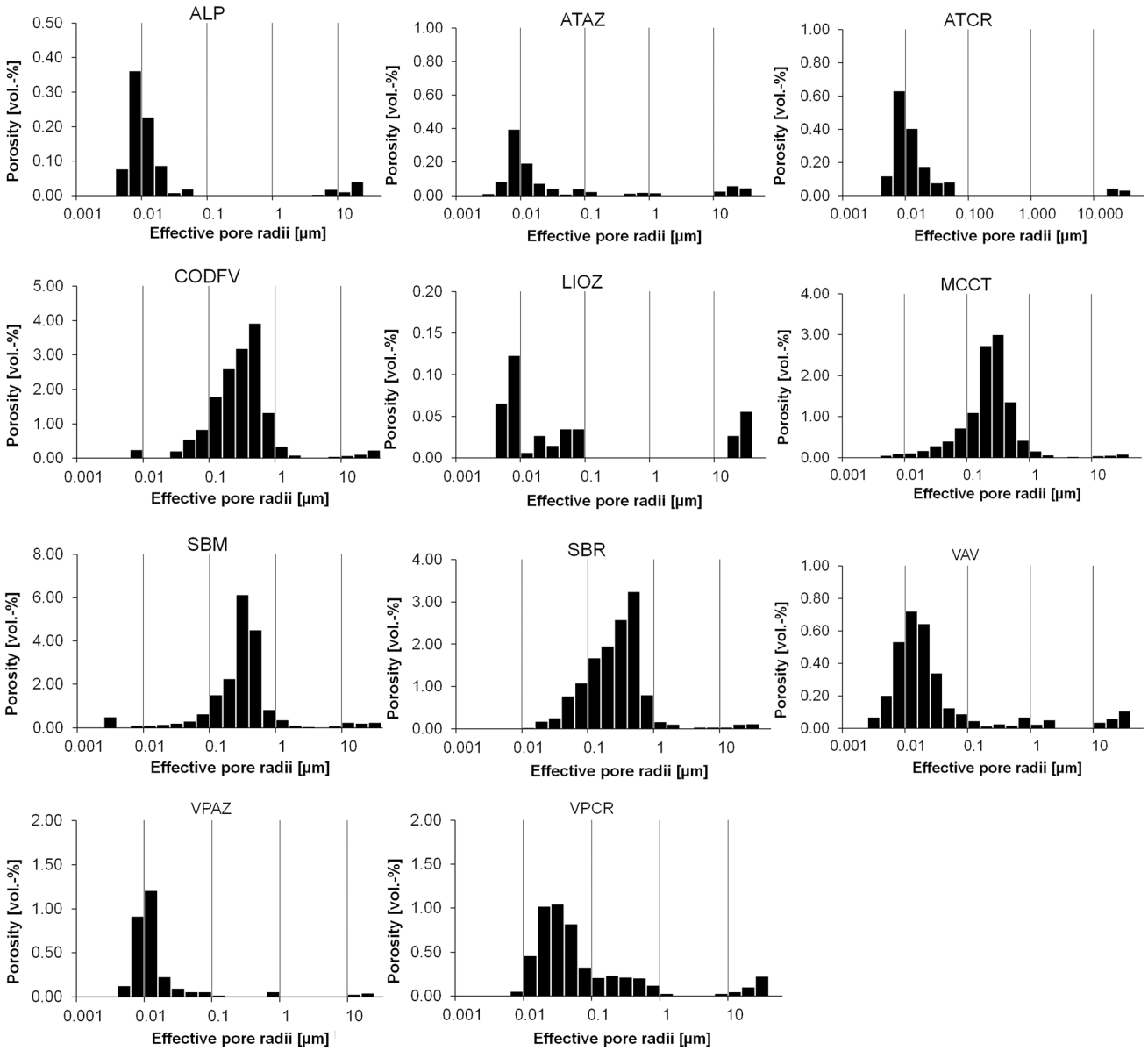

Fig. 4 The most frequent pore radii distribution of studied limestones is the unequal bimodal

from 0.37 to 0.86 kg/m^{2}h$^{1/2}$. These samples have a high percentage of macroporosity (> 1 µm), promoting the capillary imbibition and the water absorption rates (Benavente 2011; Benavente et al. 2015; Sousa et al. 2018; Nasri et al. 2019).

The values of hydric dilatation are lower than 0.09 mm/m, with the exception of the Valverde (VAV) samples which reach 0.22–0.26 mm/m (Fig. 6). Usually, limestones show low hydric dilatation because these rocks have low clay content (Siegesmund and Dürrast 2014). The presence of swelling clay is the cause for the dilation behaviour of natural stones and contributes to degradation (Wedekind et al. 2013; Cherblanc et al 2016; Nasri et al. 2019; Barnoos et al. 2020). Berthonneau et al. (2016) mention the effect of a low clay content (< 1.3%) in the macroscopic physical process of hydric dilation. Aly et al. (2018) refer to the decaying forms related with the stylolitic planes, namely the unequal thermal expansion between the stone and the filling and/or the hydric expansion of the clay content of the stylolites. Gutiérrez et al. (2012) estimated a 12% clay content in samples of Azul Valverde limestone, a variety similar to the VAV sample. The VAV sample has a high content of aluminium and silica (Table 2), which probably denotes some clay content. The dark material observed in microstylolites of the VAV sample can have some clay minerals and further investigations must be performed to investigate this issue.

Table 4 Pore radii distribution, mean pore radii and percentage of micropores (0.001 µm to 0.1 µm; % Micr) and macropores (> 0.1 µm; % Macr)

Stone	0.001–0.01 µm (%)	0.01–0.1 µm (%)	0.1–1 µm (%)	1–10 µm (%)	10–100 µm (%)	Mean (µm)	Mode (µm)	% Micr	% Macr
ALP	52.2	40.1	0.0	2.1	5.6	0.018	0.008	92.3	7.7
ATAZ	48.2	34.4	4.4	0.0	15.9	0.033	0.008	79.7	20.3
ATCR	48.2	47.1	0.0	0.0	4.7	0.016	0.008	95.3	4.7
CODFV	1.5	10.1	83.1	2.8	2.5	0.299	0.53	11.6	88.4
LIOZ	48.9	30.0	0.0	0.0	21.1	0.068	0.008	78.9	21.1
MCCT	1.3	15.2	80.5	1.8	1.2	0.218	0.33	16.5	83.5
SBM	3.1	6.9	83.2	2.6	3.4	0.298	0.33	10.0	90.0
SBR	0.0	17.3	78.7	2.3	1.7	0.258	0.53	17.3	82.7
VAV	25.5	61.1	5.1	2.2	6.1	0.030	0.013	86.6	13.4
VPAZ	37.0	58.4	2.4	0.0	2.2	0.015	0.013	95.4	4.6
VPCR	0.9	72.2	19.0	0.9	7.0	0.075	0.033	73.1	26.9

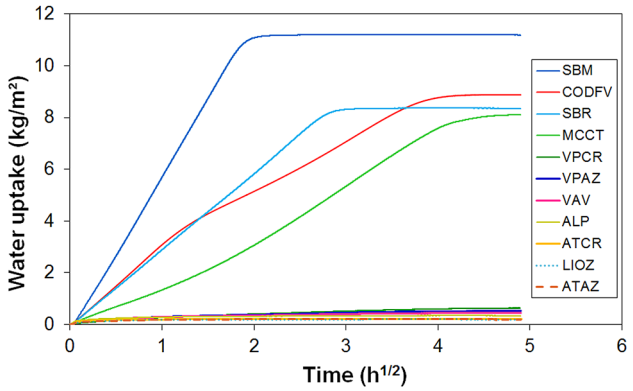

Fig. 5 Evolution of the water uptake in the selected limestones

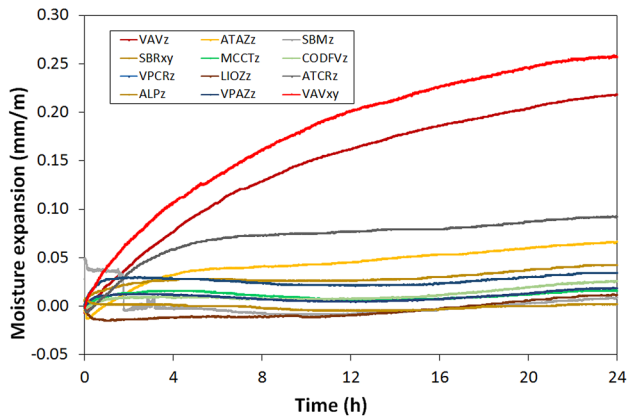

Fig. 6 Hydric expansion of the studied limestones

Ultrasonic wave velocity

The values of the compressional waves (VP) range between 4049 m/s and 5960 m/s for the samples SBM and ATAZ, respectively (see Table 5). Porosity and textural characteristics have a great effect on the ultrasonic wave velocities, and values from less than 2000 m/s to more than 6500 m/s can be found in literature, with significant variability among the specimens with high porosities (Kamh et al. 2017; Hashemi et al. 2018; Nina and Alber 2018; Freire-Lista et al. 2021). The VP depends on the density and elastic properties of the material (Rahman and Sarkar 2021). A good linear relationship between ultrasonic waves and open porosity in both dry and saturated conditions is found (Fig. 7), as observed in several investigations (Nina and Alber 2018; Nasri et al. 2019; Zenah et al. 2020). The UCS values are usually related to VP (Çobanoğlu and Çelik 2008; Rahman and Sarkar 2021), which indicates that low porous samples (CODFV, MCCT, SBM and SBR) will have poor mechanical properties in accordance with the results of similar varieties (the commercial designation is usually different from quarry to quarry) presented in the catalogues of Portuguese ornamental stones (Leite and Moura 2021; Assimagra 2021;

Table 5 Compressional wave velocities on dry and wet samples

Stone	VP dry (m/s)	VP wet (m/s)
ALP	5692	6232
ATAZ	5960	6052
ATCR	5600	5819
CODFV	4373	4452
LIOZ	5728	6014
MCCT	4536	4855
SBM	4049	4110
SBR	4321	4459
VAV	5014	5270
VPAZ	5555	5836
VPCR	5408	5674

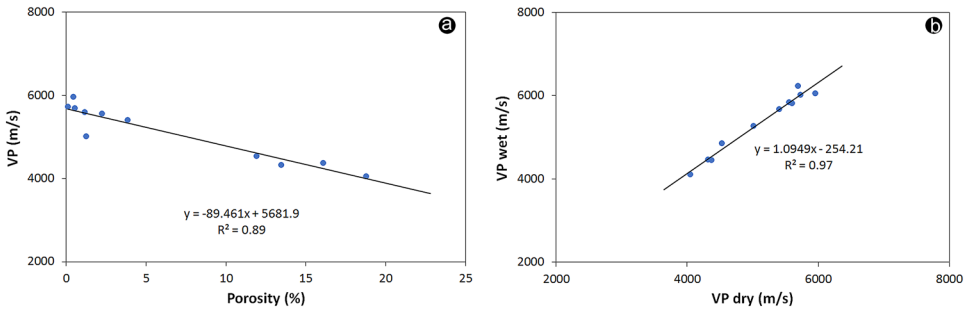

Fig. 7 Relationship between VP and porosity (**a**) and VPwet and VPdry (**b**)

Table 6 Thermal dilatation coefficient (α) and residual strain (ε_{RS}) after three dry and four wet cycles

Limestone	Condition	Average α ($\times 10^{-6}.K^{-1}$)	ε_{RS} (mm/m)
ALP	Dry	4.47	−0.01
	Wet	3.86	0.02
ATAZ	Dry	4.86	0.01
	Wet	6.46	0.28
ATCR	Dry	4.32	0.00
	Wet	3.90	0.12
CODFV	Dry	4.85	−0.01
	Wet	6.13	0.45
LIOZ	Dry	4.17	0.03
	Wet	4.35	0.35
MCCT	Dry	5.64	0.11
	Wet	4.13	0.39
SBM	Dry	5.07	0.04
	Wet	4.98	0.35
SBR	Dry	4.24	0.08
	Wet	4.20	0.35
VAV	Dry	4.82	−0.03
	Wet	4.65	0.15
VPAZ	Dry	4.74	−0.01
	Wet	3.65	−0.01
VPCR	Dry	3.80	0.02
	Wet	3.90	0.08

Solancis 2021). In those catalogues, most varieties similar to the porous limestones (CODFV, MCCT, SBM and SBR) show values of compression break load between 50 and 70 MPa, whilst the other samples showed values between 105 and 150 MPa.

Thermal dilatation

The thermal dilatation coefficient α was calculated under dry and wet conditions. The mean values range from 3.80×10^{-6} K^{-1} (VPCR) to 5.64×10^{-6} K^{-1} (MCCT) and from 3.86×10^{-6} K^{-1} (ALP) to 6.46×10^{-6} K^{-1} (ATAZ), respectively, in dry and wet states (Table 6). The mean values under dry and wet conditions are 4.63×10^{-6} K^{-1} and 4.56×10^{-6} K^{-1}, respectively, being very similar. The overall mean value of the thermal dilatation coefficient from the 22 determinations is 4.60×10^{-6} K^{-1}. Systematic investigations of limestones are still missing, but the results are according to the values previously obtained in this rock type and lower than those obtained in marbles (Siegesmund et al. 2010; Siegesmund and Dürrast 2014; Menningen et al. 2018).

The thermal dilatation ε (mm/m) as a function of temperature describes the expansion behaviour during thermal exposure and is plotted for all limestones in Figs. 8 and 9 under dry conditions. The slopes of the hysteresis curves are similar for all studied limestones and are almost linear.

The irreversible length change residual strain (εRS) under dry conditions is almost zero, ranging from −0.03 mm/m in the VAV sample to 0.11 mm/m in the MCCT sample. The negative values of residual strain near zero are not meaningful, but the lowest

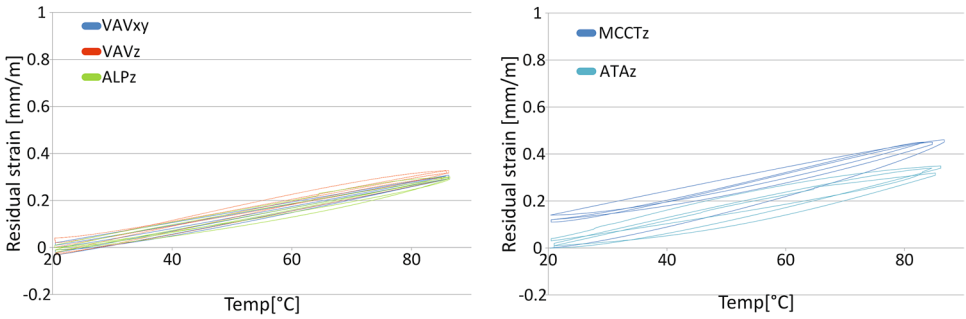

Fig. 8 Examples of thermal dilatation ε (mm/m) shown for three dry cycles (20–90–20 °C)

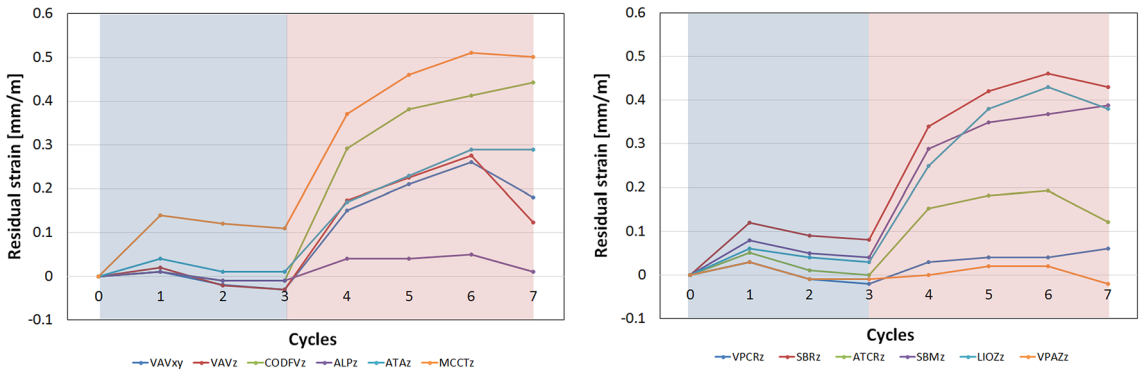

Fig. 9 Progressive increase of residual strain for 20–90–20 °C cycles of the selected samples, investigated as a function of the number of heating cycles under dry (3 cycles, blue background) and wet (4 cycles, red background) conditions

value is found in the VAV sample, which probably has some clay content. Therefore, some dehydration reaction can occur as water is present in the pores. Under wet conditions, the residual strain is usually higher with values from −0.01 mm/m for the VPAZ sample up to 0.45 mm/m for the CODFV sample. Five samples, which include the most porous ones (CODFV, LIOZ, MCCT, SBM and SBR), show a clear increase of the residual strain under wet conditions, with values in the range of 0.35–0.45 mm/m. The remaining samples have a different behaviour: ALP, VPAZ and VPCR show low variations (from −0.01 to 0.8 mm/m); ATAZ, ATCR and VAV samples depict intermediate values (from 0.12 to 0.28 mm/m). As there are only a small amount of data of the residual strain in limestones available, a comparison is difficult. The results are higher than the value of 0.07 mm/m found in Kuacker variety (Siegesmund et al. 2010) and lower than the results obtained for marbles (Siegesmund and Dürrast 2014; Menningen et al. 2018).

Bowing test

Previous results from a bowing test with 95 cycles show the absence of permanent changes in the selected limestones, except for the VAV sample (Sousa et al. 2020). During the first 24 cycles, the bowing increases continuously and reaches the value of 7 mm/m, remaining stable in the next 41 dry cycles. The next stage of the wet cycles showed a new increase of the bowing with a maximum value around 9 mm/m (Fig. 10a). Marble is the rock most prone to undergo such permanent deformation caused by the textural characteristics together with thermal strain in calcite (Siegesmund et al. 2000, 2008; Menningen et al. 2018). Weathered granites can also display bowing behaviour (Sousa et al. 2017; Siegesmund et al. 2018). Although this phenomenon is described in many rock types, there is scarce mention about limestones (Siegesmund 2008).

To assess the bowing behaviour of the VAV sample, a new bowing test was performed in three specimens, with 105 cycles, mixing wet and dry cycles. The results confirm the bending of the VAV limestone, under the combined action of heat and water (Fig. 10b). The tested specimens display

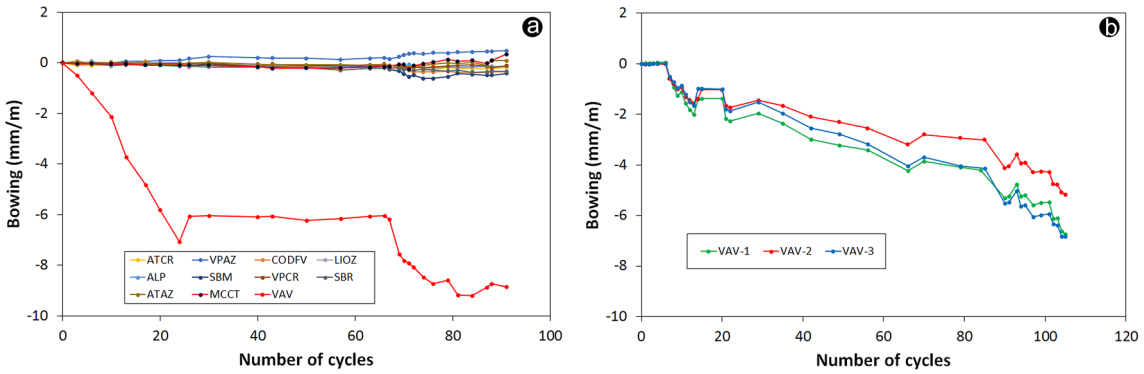

Fig. 10 Results from bowing test. **a** Results from Sousa et al. (2020); **b** New results

a similar evolution and the final bowing values range from 5.2 mm/m to 6.8 mm/m. During the first 6 dry cycles the samples stay unchanged, then deformation increases until the 13th cycle under wet conditions and finally a small recovery occurs in the next 7 dry cycles. After two wet cycles (21–22), a combination of wet/dry cycles was performed until the 84th cycle. These combined wet/dry cycles show an overall tendency of bowing increase proportional to the number of wet cycles. In fact, between cycles 22 and 29 (2 wet/5 dry) and 66 and 70 (1 wet/3 dry), a small reduction in the bending is perceived, whilst the remaining intervals of measurements, where the number of wet cycles is higher than the dry cycles, show a continuous increase of the deformation. With the exceptions of two dry cycles (92–93), the remaining cycles were performed under wet conditions and once again the velocity of bowing increased. The results reveal a clear influence of the water in the bowing evolution, being faster during successive wet cycles and slower when dry and wet cycles are interposed. It is also clear that the dry cycles only allow a small recovery of the bending.

The results are according to the behaviour of VAV limestone reported by several stoneworkers (Fig. 11). High values of bowing are frequently observed in marbles (Menningen et al. 2018), but are unknown in limestones. Furthermore, the mineralogy and texture of the selected limestones are very similar, which makes the bowing behaviour of the VAV sample strange. This samples has a residual strain value similar to the other studied limestones (see Table 6). The only different factor in the VAV sample is the microstylolites impregnated with iron oxides. The water plays an important role, since no bending occurs when dry cycles are running. Hydric expansion only is observed in the VAV sample, which is the variety with higher water loss and higher magnesium, silica, iron and aluminium content (see Table 2). Probably, some clay and iron content associated with the stylolitic planes are the reasons for the unusual bowing displayed by the VAV limestone. Gutiérrez et al. (2012) noted the presence of montmorillonite, a swelling clay mineral, in a similar limestone variety. Further studies are necessary to assess if clay swelling minerals are present in the micrite groundmass around or in the stylolitic planes. As mentioned above, a small clay content can have a deep impact on stone expansion (Berthonneau et al. 2016; Nasri et al. 2019; Barnoos et al. 2020).

Thermal shock test

The thermal shock test causes a small diminution of the VP values, which is more evident in the cycles at high temperatures (200 °C) especially in the most porous samples (Fig. 12). Fissures parallel to the cube faces and crossing all the samples are the only visible change, which is probably the cause of a fast decrease in the VP in some samples. Previous researches have shown that at temperatures up to 200 °C an adjustment process occurs, and the small cracks gradually penetrate to form larger cracks (Meng et al. 2019). Existing microcracks and open porosity are key factors for the evolution of the limestones under increasing temperatures, as well as in freezing–thawing tests (Meng et al. 2020; Uğur and Toklu 2020). Grain size, texture, and sedimentary layer can also affect the evolution of the limestones submitted to increased temperatures; however, more evident effects are mentioned for higher temperatures (Pápay and Török 2018). Wang et al. (2020) refer an increase of about 0.2% and 0.7% when heated from 25 to 200 °C and 200 to 300 °C,

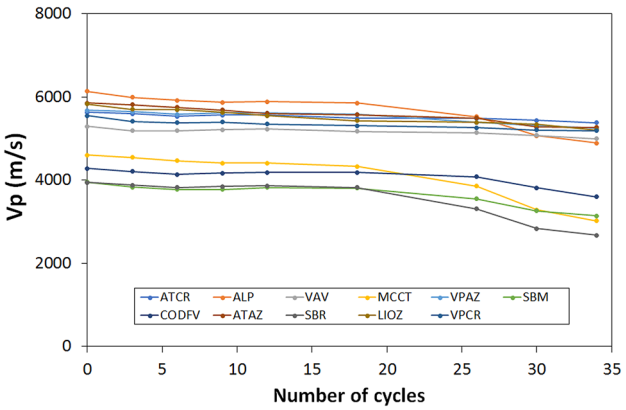

Fig. 12 Evolution of compressional wave velocity during the thermal shock test

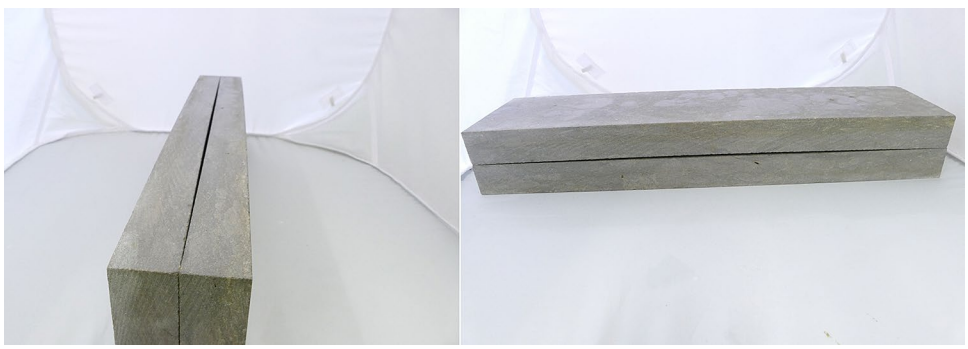

Fig. 11 Visible bowing effect on VAV samples. The bending is visible when two specimens are put together

respectively, while Meng et al. (2019) mention more evident changes after 500 °C. Bisai et al. (2020) have shown that the combined process of heating followed by liquid nitrogen quenching causes more effect at 600 °C with a reduction of about 62% in the UCS values. The results obtained in this experiment show that more massive and low porous limestones (ALP, ATAZ, ATCR, LIOZ, VAV, VPAZ, VPCR) seem to be more resistant to thermal shock, in accordance with previous properties.

Salt crystallization test

The results from the salt crystallization test depict a normal evolution of the samples weight (Fig. 13), with an increase in the first cycles following a progressive diminution according to the sample susceptibility (Nasri et al. 2019; Sousa et al. 2018). Visual inspection, used for monitoring the decay (Lubelli et al. 2018), denotes a progressive loss of material in some samples. The damage of a few millimetres can be very important when the stones are used for decorative purposes (Alves et al. 2011) where the primary consideration is the impact on aesthetic properties. After 16 cycles, only the most porous samples (CODFV, MCCT, SBM and SBR) show signs of erosion (Fig. 13), starting at the corners and the edges, but less in the sample CODFV. The other samples only lose some material in previous cracks, stylolite joints, and areas with heterogeneities as large elements or marked sedimentary layering (Fig. 14). However, the loss of material is balanced by the accumulation inside the porous network (Nasri et al. 2019) and only after around the 40th cycle weight diminution below the initial values is evident. The most porous samples have a maximum weight increase between 4 and 8%, whilst the others increase below 1%. The maximum loss is shown by the samples with high porosity as follows: SBR lost 80% on cycle 54, the SBM lost 57% in 62 cycles, MCCT lost 53% in 99 cycles and COFV lost only 1.5% in 99 cycles. The sample LIOZ lost 0.5% related

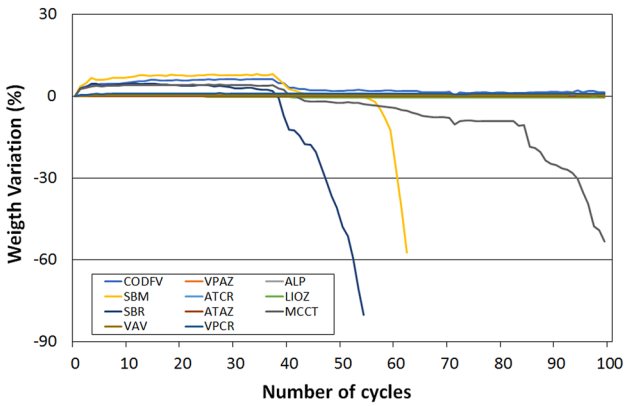

Fig. 13 Weight variation during the salt crystallization test

to detachment of small pieces, while the remaining samples still have positive values at the end of the test (99 cycles), ranging from 0.1% for the ATAZ sample to 0.9% for the VPCR sample. The real weight loss is higher as the weight of salt crystallized inside the samples and can be higher than the weight decrease (see Vázquez et al. 2013).

A wide range of effects can be perceived from literature review, varying from high loss to small or any change (Alves et al. 2011; Vázquez et al. 2013; Ruffolo et al 2017) mainly as a consequence of porosity and pore network. The effect of salt is related to porosity, indicating that stones with a larger quantity of pores have more contact surfaces between crystals and pore walls. In these surfaces, more crystallization pressure is exerted and more damage occurs (Espinosa-Marzal and Scherer 2008). The sample SBR starts losing weight earlier than sample SBM, despite their lower porosity (SBR 13.4%; SBM 18.8%). The high mode of pore radii in SBR sample (SBM 0.33 µm; SBR 0.53 µm) and the slight impregnation by yellowish hydrated iron oxides of the peloids in the SBM sample can justify the fast deterioration of SBR. In this regard, the result of CODFV is surprisingly better than expected considering its high porosity and pore radii distribution. Possible causes are the abundant sparitic cement, which prevents the detachment of grains and cementation of loose particles by salt (Lubelli et al. 2018). Sample preparation could infill the pores by smaller particles from the disaggregation of the limestone itself. Urosevic et al. (2013) point out differences in sea spray ageing test as a consequence of the reduction of the interconnectivity and open porosity due to polishing. Such causes are not reasonable to justify the results of CODFV and more studies are necessary to understand the behaviour of this stone under salt action.

The stones can be ranked according to their response to the salt crystallization in the test (Lubelli et al. 2014). However, not only the weight variation should be considered in this evaluation of cases like the CODFV sample (see Lubelli et al. 2018). Furthermore, when stones are used for their aesthetic appeal, even small damages need to be considered. So considering the results of the salt test, the most porous stones (CODFV, MCCT, SBM and SBR) should be considered as susceptible to salt action, whilst the other samples are resistant.

Summary and conclusions

Eleven commercial varieties of Portuguese limestones were studied to assess the influence of the textural characteristics in the physical–mechanical properties and durability behaviour. Some important conclusions can be drawn.

- The selected varieties have a wide range of petrographic features, according to the grain size, matrix and cement

Fig. 14 Evolution of selected samples during the salt test

type (micrite/sparite) and abundance of allochems. Two main groups were identified regarding the texture/petrography, one with the compact micritic limestones classified as pelagic mudstones or peloidal wackestones, and the other with grainstones sparitic varieties such as the peloidal, bioclastic and ooid grainstones. The chemical composition of the studied limestones is very similar; however, the Vidraço Azul Valverde (VAV) limestone stands out showing a high quantity of magnesium. In fact, VAV limestone shows 90.9% of calcite, whilst the other limestones have values between 94.5% and 98.4%. With magnesium carbonate, the opposite happens; the VAV limestone shows a value of 4.8%, while the other limestones have values in the range 1.3%—2.6%.

- The matrix density is close to the density of calcite, since it is the main component of the limestones studied. The bulk density varies slightly between 2.61 and 2.71 g/cm^3 in eight samples and is lower with 2.22–2.39 g/cm^3 in

four grainstone varieties because of the higher percentage of void space.

- The values of porosity show a wide range, from 0.11% to 18.80%, reflecting the span of rock types and related textures. Since the porosity is an excellent indicator of weathering, the high values can be used as an alert for the potentially low durability of the most porous varieties in some applications/environmental conditions. The interconnected porosity shows an unequal bimodal distribution with most of the pores distributed in the range between 0.01 µm and 0.8 µm and some pores with 10–50 µm. The clastic and most porous varieties (CODFV, MCCT, SBM and SBR) have larger pore sizes and a higher percentage of macroporosity (> 0.1 µm). Besides a higher total porosity, the most porous samples have a higher potential of water absorption, which has been confirmed by the results of capillary water absorption. In fact, the most porous samples show values of capillary water absorption between 1.59 and 5.50 kg/$m^2h^{1/2}$, whilst the remaining samples have values in the range 0.37–0.86 kg/$m^2h^{1/2}$.
- The values of hydric dilatation are lower than 0.09 mm/m, with the exception of the Valverde (VAV) samples which reach 0.22–0.26 mm/m (Fig. 6). The hydric expansion of the VAV sample together with their high content of aluminium and silica (when compared with other studied limestones) show that some clay content is present.
- The compressional wave velocities range between 4049 m/s and 5960 m/s, having a good linear relationship with the open porosity and the available data of uniaxial compressive strength. Therefore, the compressional wave velocity is a good and non-destructive index to assess the suitability of limestone as building material.
- The values of the thermal dilatation coefficient under dry and wet conditions are very similar, with mean values of the 11 samples of 4.63×10^{-6} K^{-1} and 4.56×10^{-6} K^{-1}, respectively. Under dry conditions, the residual strain is almost zero and increases under wet conditions especially in the most porous varieties, reaching the highest value (0.45 mm/m) in the CODFV sample.
- The results of the bowing test confirm the bending of the VAV limestone, under the combined action of heat and water, with final bowing values in the range 5.2–6.8 mm/m. The results reveal a clear influence of the water in the bowing evolution, being faster during successive wet cycles and slower when dry and wet cycles are intercalated. The residual strain of the VAV sample is similar to the other studied limestones. Probably, some clay and iron contents associated with the stylolitic planes are the reason for the unusual bowing displayed.
- The thermal shock test causes a small diminution of the VP values, which is more evident in the cycles at high temperatures (200 °C) especially in the most porous samples. For the normal applications, the limestones will not be affected by the action of the temperature.
- The results from the salt crystallization test depict a normal evolution of the sample weight, with an increase in the first cycle following a progressive diminution according to the sample susceptibility. The most porous stones (CODFV, MCCT, SBM and SBR) should be considered as susceptible to salt action, whilst the other samples are resistant.

From the main conclusions enumerated above, the importance of the texture and the petrographic features are obvious in the porosity of limestones. The compact micritic samples have lower porosities than the grainstone sparitic varieties. Porosity is the key factor in the limestone behaviour, affecting the water absorption and durability under salt action.

Notwithstanding the high values of porosity, the limestones can be used as long as they meet the standards for the several applications and resist the environmental conditions of their application. This already has been done by the extracting and processing companies. This is a decisive factor as a wrong application can have serious consequences, and decades of marketing diplomacy can be lost by a single building where the stone was not judiciously selected.

Evidences of bowing in limestones are scarce and have low values, but the bending shown by the VAV samples is outstanding. Further studies are necessary to assess if clay swelling minerals and iron oxides are present in the micrite groundmass around or in the stylolitic planes which are typical in the studied samples. Additionally, the study of the sedimentary layering and their variation in the outcrops/quarries is important to define the areas of rock mass more prone to bowing. Meanwhile, it is suggested that this variety should not be used in external applications under wet conditions and effect of temperature.

Acknowledgements This study was supported by the Fundação para a Ciência e a Tecnologia in the frame of the UIDB/00073/2020 and UIDP/00073/2020 projects of the I&D unit Geosciences Center (CGEO). The authors are grateful to Solancis for supply of the samples used in this research.

References

Agan C (2016) A preliminary study on the conservation and polishing performance of Sanliurfa limestones as a traditional building material. Bull Eng Geol Environ 75:13–25. https://doi.org/10.1007/s10064-015-0729-6

Akram MS, Farooq S, Naeem M, Ghazi S (2017) Prediction of mechanical behaviour from mineralogical composition of Sakesar limestone, Central Salt Range, Pakistan. Bull Eng Geol Environ 76:601–615. https://doi.org/10.1007/s10064-016-1002-3

Alves C, Figueiredo C, Maurício A, Braga MAS, Aires-Barros L (2011) Limestones under salt decay tests: assessment of pore

network-dependent durability predictors. Environ Earth Sci 63:1511–1527. https://doi.org/10.1007/s12665-011-0915-1

Aly N, Wangler T, Török Á (2018) The effect of stylolites on the deterioration of limestone: possible mechanisms of damage evolution. Environ Earth Sci 77:565. https://doi.org/10.1007/s12665-018-7746-2

Anovitz LM, Cole DR (2015) Characterization and analysis of porosity and pore structures. Rev Mineral Geochem 80:61–164. https://doi.org/10.2138/rmg.2015.80.04

Arman H, Abdelghany O, Saima MA et al (2021) Petrological control on engineering properties of carbonate rocks in arid regions. Bull Eng Geol Environ. https://doi.org/10.1007/s10064-021-02211-8

Assimagra (2021) Portuguese Stone Catalogue. https://www.assimagra.pt/3d-flip-book/catalogo-da-pedra-portuguesa/. Accessed in 7th July 2021

Barnoos V, Oudbashi O, Shekofteh A (2020) The deterioration process of limestone in the Anahita Temple of Kangavar (West Iran). Heritage Sci 8:66. https://doi.org/10.1186/s40494-020-00411-1

Barroso CE, Oliveira DV, Ramos LF (2018) Vernacular schist farm walls: materials, construction techniques and sustainable rebuilding solutions. J Build Eng 15:334–352. https://doi.org/10.1016/j.jobe.2017.12.001

Benavente D (2011) Why pore size is important in the deterioration of porous stones used in the built heritage. Macla 15:41–42

Benavente D, Pla C, Cueto N, Galvañ S, Martínez-Martínez J, García-del-Cura MA, Ordóñez S (2015) Predicting water permeability in sedimentary rocks from capillary imbibition and pore structure. Eng Geol 195:301–311

Berthonneau J, Grauby O, Ferrage E, Vallet JM, Bromblet P, Dessandier D, Chaudanson D, Baronnet A (2014) Impact of swelling clays on the spalling decay of building limestones: insights from X-ray diffraction profile modeling. Eur J Miner 26:643–656. https://doi.org/10.1127/0935-1221/2014/0026-2393

Berthonneau J, Bromblet P, Cherblanc F, Ferrage E, Vallet J-M, Grauby O (2016) The spalling decay of building bioclastic limestones of Provence (South East of France): From clay minerals swelling to hydric dilation. J Cult Herit 17:53–60. https://doi.org/10.1016/j.culher.2015.05.004

Bisai R, Palaniappan SK, Pal SK (2020) Effects of high-temperature heating and cryogenic quenching on the physico-mechanical properties of limestone. SN Appl Sci 2:158. https://doi.org/10.1007/s42452-020-1944-8

Carvalho JMF, Lisboa JV, Moura AC, Carvalho C, Sousa LMO, Leite MM (2013) Evaluation of the Portuguese ornamental stone resources. Key Eng Mater 548:3–9

Carvalho C, Silva Z, Simão J (2018) Evaluation of Portuguese limestones' susceptibility to salt mist through laboratory testing. Environ Earth Sci 77:523. https://doi.org/10.1007/s12665-018-7670-5

Carvalho JMF, Sampaio J, Machado S, Midões C, Prazeres C, Sardinha R (2014) Caracterização e valorização da área de intervenção específica de Pé de Pedreira. Cluster da Pedra Natural. 237 pp

Carvalho JMF (2013) Tectónica e caraterização da fraturação do Maciço Calcário Estremenho, Bacia Lusitaniana. Contributo para a prospeção de rochas ornamentais e ordenamento da atividade extrativa. Ph.D. Thesis, Universidade de Lisboa (in Portuguese)

Çelik MY, Kaçmaz AU (2016) The investigation of static and dynamic capillary by water absorption in porous building stones under normal and salty water conditions. Environ Earth Sci 75:307. https://doi.org/10.1007/s12665-015-5132-x

Cherblanc F, Berthonneau J, Bromblet P, Huon V (2016) Influence of water content on the mechanical behaviour of limestone: role of the clay minerals content. Rock Mech Rock Eng 49:2033–2042. https://doi.org/10.1007/s00603-015-0911-y

Çobanoğlu İ, Çelik SB (2008) Estimation of uniaxial compressive strength from point load strength, Schmidt hardness and P-wave velocity. Bull Eng Geol Environ 67:491–498. https://doi.org/10.1007/s10064-008-0158-x

Dunham RJ (1962) Classification of carbonate rocks according to depositional textures. In: Ham WE (Ed.), Classification of Carbonate Rocks: American Association of Petroleum Geologists, Memoir 1, 108–121

DIN EN 14579 (2004) Prüfverfahren für Naturstein - Bestimmung der Geschwindigkeit der Schallausbreitung; Deutsche Fassung EN 14579:2004

DIN EN 16306:2013–05 (2013) Prüfverfahren für Naturstein_-Bestimmung der Beständigkeit von Marmor bei zyklischer Belastung mit Wärme und Feuchtigkeit; Deutsche Fas-sung EN_16306:2013. Beuth Verlag GmbH, Berlin https://doi.org/10.31030/1910871.

Eslami J, Grgic D, Hoxha D (2010) Estimation of the damage of a porous limestone from continuous (P- and S-) wave velocity measurements under uniaxial loading and different hydrous conditions. Geophys J Int 183:1362–1375. https://doi.org/10.1111/j.1365-246X.2010.04801.x

Espinosa-Marzal RM, Scherer GW (2008) Crystallization of sodium sulfate salts in limestone. Environ Geol 56:605–621. https://doi.org/10.1007/s00254-008-1441-7

Espinosa-Marzal RM, Hamilton A, McNall M, Whitaker K, Scherer GW (2011) The chemomechanics of crystallization during rewetting of limestone impregnated with sodium sulfate. J Mater Res 26(12):1472–1481. https://doi.org/10.1557/jmr.2011.137

Feijoo J, Nóvoa XR, Rivas T (2017) Electrokinetic treatment to increase bearing capacity and durability of a granite. Mater Struct 50:251. https://doi.org/10.1617/s11527-017-1123-6

Fereidooni D (2019) Khajevand R (2019) Utilization of the accelerated weathering test method for evaluating the durability of sedimentary rocks. Bull Eng Geol Environ 78:2697–2716. https://doi.org/10.1007/s10064-018-1267-9

Folk RL (1962) Spectral subdivision of limestones types. In Ham WE (Ed.), Classification of Carbonate Rocks: American Association of Petroleum Geologists, Memoir 1, 62–84

Freire-Gormaly M, Ellis JS, MacLean HL, Bazylak A (2015) Pore structure characterization of Indiana Limestone and Pink Dolomite from pore network reconstructions. Oil Gas Sci Technol Rev IFP Energ Nouvelles. https://doi.org/10.2516/ogst/2015004

Freire-Lista DM, Sousa L, Carter R, Al-Na'īmī F (2021) Petrography and petrophysical characterisation of the heritage stones of Fuwairit Archaeological Site (NW Qatar) and their historical quarries: implications for heritage conservation. Episodes 44(1): 43–58. https://doi.org/10.18814/epiiugs/2020/0200s12.

Grelk B, Goltermann P, Schouenborg B, Koch A, Alnaes L (2004) The laboratory testing of potential bowing and expansion of marble. In: Proceedings of the international conference on dimension stone 2004, 14–17 June 2004, Prague, pp 253–259

Gutiérrez J, Mas A, Gil E, Galvañ V (2012) Clay-related damage in rainscreen walls built with natural stone coverings. Constr Build Mater 29:357–367. https://doi.org/10.1016/j.conbuildmat.2011.10.060

Hashemi M, Bashiri Goudarzi M, Jamshidi A (2018) Experimental investigation on the performance of Schmidt hammer test in durability assessment of carbonate building stones against freeze–thaw weathering. Environ Earth Sci 77:684. https://doi.org/10.1007/s12665-018-7874-8

Hu Z, Klaver J, Schmatz J, Dewanckele J, Littke R, Krooss BM, Amann-Hildenbrand A (2020) Stress sensitivity of porosity and permeability of Cobourg limestone. Eng Geol. https://doi.org/10.1016/j.enggeo.2020.105632

Jensen LRD, Friis H, Fundal E, Møller P, Jespersen M (2010) Analysis of limestone micromechanical properties by optical microscopy. Eng Geol 110: 43–50. https://doi.org/10.1016/j.enggeo.2009.10.004

Kamh GME, Koltuk S (2017) Ismael H (2017) Refinement of categorization and scaling of weathering-related damage to natural stone: case study on oolitic limestone from El-Shatbi Tombs (Egypt). Bull Eng Geol Environ 76:39–57. https://doi.org/10.1007/s10064-016-0946-7

Karagiannis N, Karoglou M, Bakolas A, Moropoulou A (2016) Building materials capillary rise coefficient: concepts, determination and parameters involved. In: Delgado J (ed) New approaches to building pathology and durability. Building pathology and rehabilitation, vol 6. Springer, Singapore

Klopfer H (1985) Feuchte. In: Lutz et al (eds) Lehrbuch der Bauphysik. Teubner, Stuttgart

Koch A, Siegesmund S (2002) Bowing of marble panels: on-site damage analysis from the Oeconomicum building at Goettingen (Germany). Geol Soc Lond Spec Public 205(1):299–314

Koch A, Siegesmund S (2004) The combined effect of moisture and temperature on the anomalous expansion behaviour of marble. Environ Geol 46:350–363

Korkanç M, İnce İ, Hatır ME, Tosunlar MB (2021) Atmospheric and anthropogenic deterioration of the İvriz rock monument: Ereğli-Konya, Central Anatolia, Turkey. Bull Eng Geol Environ 80:3053–3063. https://doi.org/10.1007/s10064-021-02105-9

Leite MRM, Moura AC (2021) Catalogue of Portuguese Ornamental Stones. INETI. Published online in https://rop.lneg.pt/rop/images/intro/intr_en.php. Accessed in 23th June 2021

López-Doncel RA, Wedekind W, Cardona-Velázquez N, González-Sámano PS, Dohrmann R, Siegesmund S, Pötzl C (2016) Geological studies on volcanic tuffs used as natural building stones in the Historical Center of San Luis Potosí, Mexico. In: Hughes JJ, Howind T (eds) Science and art: a future for stone. Proceedings of the 13th international congress on the deterioration and conservation of stone, pp 107–105. University of the West of Scotland, Paisley

Lubelli B, Cnudde V, Diaz-Goncalves T et al (2018) Towards a more effective and reliable salt crystallization test for porous building materials: state of the art. Mater Struct 51:55

Lubelli B, van Hees RPJ, Nijland TG (2014) Salt crystallization damage: how realistic are existing ageing tests? AMS '14 Proceedings of the International Conference on Ageing of Materials & Structures, Delft, The Netherlands, pp 103–111

Majeed Y, Abu Bakar MZ, Butt IA (2020) Abrasivity evaluation for wear prediction of button drill bits using geotechnical rock properties. Bull Eng Geol Environ 79:767–787. https://doi.org/10.1007/s10064-019-01587-y

Matović V, Ćalić TV (2016) Mesozoic carbonate rocks in Serbia used as dimension stone. Bull Eng Geol Environ 75:1–12. https://doi.org/10.1007/s10064-015-0722-0

Meng Q, Zhang M, Han L, Chen Y (2019) Experimental research on the influence of loading rate on the mechanical properties of limestone in a high-temperature state. Bull Eng Geol Environ 78:3479–3492. https://doi.org/10.1007/s10064-018-1332-4

Meng QB, Wang CK, Liu JF et al (2020) Physical and micro-structural characteristics of limestone after high temperature exposure. Bull Eng Geol Environ 79:1259–1274. https://doi.org/10.1007/s10064-019-01620-0

Menningen J, Siegesmund S, Lopes L, Martins R, Sousa L (2018) The Estremoz marbles: an updated summary on the geological, mineralogical and rock physical characteristics. Environ Earth Sci 77:191. https://doi.org/10.1007/s12665-018-7328-3

Molina E, Benavente D, Sebastian E, Cultrone G (2015) The influence of rock fabric in the durability of two sandstones used in the Andalusian Architectural Heritage (Montoro and Ronda, Spain). Eng Geol 197:67–81. https://doi.org/10.1016/j.enggeo.2015.08.009

Montani C 2017 XXVIII report marble and stones in the world 2016. Ed. Aldus, Carrara, Italy.

Mustafa S, Khan MA, Khan MR, Sousa LMO, Hameed F, Mughal MS, Niaz A (2016) Building stone evaluation—A case study of the sub-Himalayas, Muzaffarabad region, Azad Kashmir, Pakistan. Eng Geol 209:56–69. https://doi.org/10.1016/j.enggeo.2016.05.007

Nabawy BS, El Aal AA (2019) Impacts of the petrophysical and diagenetic aspects on the geomechanical properties of the dolomitic sequence of Gebel El-Halal, Sinai. Egypt Bull Eng Geol Environ 78:2627–2640. https://doi.org/10.1007/s10064-018-1264-z

Nasri F, Boumezbeur A, Benavente D (2019) Influence of the petrophysical and durability properties of carbonate rocks on the deterioration of historic constructions in Tebessa (northeastern Algeria). Bull Eng Geol Environ 78:3969–3981. https://doi.org/10.1007/s10064-018-1410-7

Nina H, Alber M (2018) Variation of laboratory test results with specimen size in carbonates of Bavarian Malm. Paper presented at the ISRM European Rock Mechanics Symposium - EUROCK 2018, St. Petersburg, Russia

Özvan A, Direk N (2021) The relationships among different abrasion tests on deteriorated and undeteriorated rocks. Bull Eng Geol Environ 80:1745–1756. https://doi.org/10.1007/s10064-020-02041-0

Pápay Z (2018) Török Á (2018) Effect of thermal and freeze-thaw stress on the mechanical properties of porous limestone. Periodica Polytechnica Civil Eng 62:423–428. https://doi.org/10.3311/PPci.11100

Rahman T, Sarkar K (2021) Lithological control on the estimation of uniaxial compressive strength by the P-wave velocity using supervised and unsupervised learning. Rock Mech Rock Eng. https://doi.org/10.1007/s00603-021-02445-8

Randazzo L et al (2020) (2021) Pore Structure and Water Transfer in Pietra d'Aspra Limestone: A Neutronographic Study. Appl Sci 10:6745. https://doi.org/10.3390/app10196745

Ruedrich J, Siegesmund S (2007) Salt and ice crystallisation in porous sandstones. Environ Geol 52(2):225–249

Ruffolo SA, La Russa MF, Ricca M et al (2017) (2017) New insights on the consolidation of salt weathered limestone: the case study of Modica stone. Bull Eng Geol Environ 76:11–20. https://doi.org/10.1007/s10064-015-0782-1

La Russa MF, Ruffolo SA, Belfiore CM, Aloise P, Randazzo L, Rovella N, Pezzino A, Montana G (2013) Study of the effects of salt crystallization on degradation of limestone rocks. Periodico Mineral 82(1):113–127. https://doi.org/10.2451/2013PM0007

Santos I, Sousa L, Lourenço J (2018) Granite resources evaluation - example of an extraction area in North of Portugal. Environm Earth Sci 77:608. https://doi.org/10.1007/s12665-018-7780-0

Shushakova V, Fuller ER, Heidelbach F, Mainprice D, Siegesmund S (2013) Marble decay induced by thermal strains: simulations and experiments. Environ Earth Sci 69(4):1281–1297

Siegesmund S, Ullemeyer K, Weiss T, Tschegg EK (2000) Physical weathering of marbles caused by anisotropic thermal expansion. Int J Earth Sci 89(1):170–182

Siegesmund S, Rüdrich J, Koch A (2008) Marble bowing: comparative studies of three different public building façades. Environ Geol 56(3–4):473–494

Siegesmund S, Grimm WD, Dürrast H, Ruedrich J (2010) Limestones in Germany used as building stones: an overview. Geol Soc Lond Special Publ 331(1):37–59

Siegesmund S, Dürrast H (2014) Physical and mechanical properties of the rocks. In: Siegesmund S, Snethlage R (eds) Stone in architecture. Properties, durability, 5th edn. Springer

Siegesmund S (2008) Neue Steine und alte Sorgen—Fassadenplatten aus Naturstein: Sicherheitsrisiken und Sanierungsstrategien. In: H. Venzmer (Hrsg.) 19. Hanseatische Sanierungstage Bauphysik und Bausanierung Heringsdorf 2008, S. 17–27, Beuth Verlag, Berlin

Siegesmund S, Sousa L, Knell C (2018) Thermal expansion of granitoids. Environ Earth Sci 77:41. https://doi.org/10.1007/s12665-017-7119-2

Silva Z (2017) The Portuguese Lioz, a monumental limestone. Geophysical Research Abstracts. Vol. 19, EGU2017–9019.

Solancis (2021). Stone properties. http://www.solancis.com/stones. Accessed in 25th June 2021

Sousa LMO, Oliveira AS, Alves IMC (2016) Influence of fracture system on the exploitation of building stones: the case of the Mondim de Basto granite (north Portugal). Environ Earth Sci 75:39. https://doi.org/10.1007/s12665-015-4824-6

Sousa L, Siegesmund S, Wedekind W (2018) Salt weathering in granitoids: an overview on the controlling factors. Environm Earth Sci 77:502. https://doi.org/10.1007/s12665-018-7669-y

Sousa L, Barabasch J, Stein K-J, Siegesmund S (2017) Characterization and quality assessment of granitic building stone deposits: a case study of two different Portuguese granites. Eng Geol 221:29–40. https://doi.org/10.1016/j.enggeo.2017.01.030

Sousa L, Menningen J, Sigesmund S (2020) Notes of a bowing behavior on limestone. In Siegesmund S, Middendorf B (Ed.), Monument Future: Decay and Conservation of Stone Proceedings of the 14th International Congress on the Deterioration and Conservation of Stone, Mitteldeuscher Verlag, pp. 145–150. ISBN: 987–3–96311–172–3

Strohmeyer D (2003) Gefügeabhängigkeit technischer Gesteinseigenschaften. Dissertation, Universität Göttingen, 254 S

Stück H, Plagge R, Siegesmund S (2013) Numerical modeling of moisture transport in sandstone: the influence of pore space, fabric and clay content. Environ Earth Sci 69(4):1161–1187. https://doi.org/10.1007/s12665-013-2405-0

Szemerey-Kiss B, Török Á (2017) Failure mechanisms of repair mortar stone interface assessed by pull-off strength tests. Bull Eng Geol Environ 76:159–167. https://doi.org/10.1007/s10064-016-0964-5

Taghipour M, Nikudel MR, Farhadian MB (2017) Engineering properties and durability of limestones used in Persepolis complex, Iran, against acid solutions. Bull Eng Geol Environ 75:967–978. https://doi.org/10.1007/s10064-015-0821-y

Tomašić I, Lukić D, Peček N, Kršinić A (2011) Dynamics of capillary water absorption in natural stone. Bull Eng Geol Environ 70:673–680. https://doi.org/10.1007/s10064-011-0355-x

Török A, Szemerey-Kiss B (2019) Freeze-thaw durability of repair mortars and porous limestone: compatibility issues. Prog Earth Planet Sci 6:42. https://doi.org/10.1186/s40645-019-0282-1

Tugrul A, Zarif I (2000) Engineering aspects of limestone weathering in Istanbul, Turkey. Bull Eng Geol Env 58:191–206. https://doi.org/10.1007/s100640050075

Turgut P, Yesilnacar MI, Bulut H (2008) Physico-thermal and mechanical properties of Sanliurfa limestone, Turkey. Bull Eng Geol Environ 67:485–490. https://doi.org/10.1007/s10064-008-0145-2

Uğur İ, Toklu HÖ (2020) Effect of multi-cycle freeze-thaw tests on the physico-mechanical and thermal properties of some highly porous natural stones. Bull Eng Geol Environ 79:255–267. https://doi.org/10.1007/s10064-019-01540-z

Unterwurzacher M, Mirwald PW (2008) Initial stages of carbonate weathering: climate chamber studies under realistic pollution conditions. Environ Geol 56:507–519. https://doi.org/10.1007/s00254-008-1440-8

Urosevic M, Sebastián E, Cardell C (2013) An experimental study on the influence of surface finishing on the weathering of a building low-porous limestone in coastal environments. Eng Geol 154:131–141. https://doi.org/10.1016/j.enggeo.2012.12.013

Van Stappen JF, De Kock T, De Schutter G (2019) Cnudde V (2019) Uniaxial compressive strength measurements of limestone plugs and cores: a size comparison and X-ray CT study. Bull Eng Geol Environ 78:5301–5310. https://doi.org/10.1007/s10064-018-01448-0

Vázquez P, Alonso FJ, Carrizo L, Molina E, Cultrone G, Blanco M, Zamora I (2013) Evaluation of the petrophysical properties of sedimentary building stones in order to establish quality criteria. Constr Build Mater 41:868–878. https://doi.org/10.1016/j.conbuildmat.2012.12.026

Vázquez P, Menéndez B, Denecker MF, Thomachot-Schneider C (2015) Comparison between petrophysical properties, durability and use of two limestones of the Paris region. In: Přikryl R, Török A, Gómez-Heras M, Miskovsky K, Theodoridou M (eds) Sustainable use of traditional geomaterials in construction practice. Geol Soc Lond Spec Publ 416 https://doi.org/10.1144/SP416.15

Wang S, Sun Q, Wang N, Yang L (2020) Variation in the dielectric constant of limestone with temperature. Bull Eng Geol Environ 79:1349–1355. https://doi.org/10.1007/s10064-019-01647-3

Wedekind W, López-Doncel R, Dohrmann R, Kocher M, Siegesmund S (2013) Weathering of volcanic tuff rocks caused by moisture expansion. Environ Earth Sci 69:1203–1224. https://doi.org/10.1007/s12665-012-2158-1

Weiss T, Siegesmund S, Kirchner DT, Sippel J (2004) Insolation weathering and hygric dilatation: two competitive factors in stone degradation. Environ Geol 46(3–4):402–413

Yagiz S (2011) Correlation between slake durability and rock properties for some carbonate rocks. Bull Eng Geol Environ 70:377–383. https://doi.org/10.1007/s10064-010-0317-8

Yarahmadi R, Bagherpour R, Taherian S-G, Sousa LMO (2018) Discontinuity modelling and rock block geometry identification to optimize production in dimension stone quarries. Eng Geol 232:22–33. https://doi.org/10.1016/j.enggeo.2017.11.006

Yarahmadi R, Bagherpour R, Khademian A, Sousa LMO, Almasi SN, Esfahani MM (2019a) Determining the optimum cutting direction in granite quarries through experimental studies: a case study of a granite quarry. Bull Eng Geol Env 78:459–467. https://doi.org/10.1007/s10064-017-1158-5

Yarahmadi R, Bagherpour R, Taherian S-G, Sousa LMO (2019b) A new quality factor for the building stone industry: a case study of stone blocks, slabs, and tiles. Bull Eng Geol Env 78:533–542. https://doi.org/10.1007/s10064-017-1040-5

Yaşar E, Erdoğan Y, Güneyli H (2008) Determination of the thermal conductivity from physico-mechanical properties. Bull Eng Geol Environ 67:219–225. https://doi.org/10.1007/s10064-008-0126-5

Zammit T, Cassar J (2017) Investigating possible correlations between the porosimetry and insoluble residue content of Malta's Lower Globigerina Limestone. Bull Eng Geol Environ 76:59–70. https://doi.org/10.1007/s10064-015-0817-7

Zeisig A, Siegesmund S, Weiss T (2002) Thermal expansion and its control on the durability of marbles. Geol Soc Lond Spec Publ 205(1):65–80

Zenah J, Görög P, Török A (2020) Stability of underground excavation in porous limestone: influence of water content. Acta Montanistica Slovaca 25 (3): 337–349. https://doi.org/10.46544/AMS.v25i3.7